

Numerical Study of High-Energy Collisions Inside the Shock Wave in a Gas Mixture

F. Tcheremissine, O. Dodulad, and Yu. Kloss

Introduction

One considers a phenomenon that has been observed in some experimental works [1, 2], confirmed by an analysis based on the assumption of a bimodal shape of the distribution functions inside the SW [1] and by computations using the Monte Carlo simulation method [3–5]. The phenomenon consists of an excess of high-energy molecular collisions inside the SW in a gas mixture compared to the value behind the wave. It was found that the excess of such collisions is most expressed for gas mixtures with high difference of concentrations and molecular masses of the components.

In this paper the study is made by deterministic solution of the Boltzmann kinetic equation with the application of the conservative projection method [6]. We consider the binary mixture with highly different molecular masses and concentrations and apply a special version of the method that was developed for the case of high ratio of molecular masses [7]. The method permits to obtain accurate solution of the kinetic equation without the statistical noise inherent in the statistical simulation approaches. Previously, the method was applied in a number of simulations of slow flows inside micro-devices for the problem of gas separation. To prove its accuracy in the considered case of the supersonic flow in the shock wave problem, some preliminary tests and comparisons were performed.

Statement of the Problem and Testing of the Accuracy

The SW structure is formed by evolution of the initial discontinuity at $x = 0$ that separates the gas with parameters related by Rankin–Hugoniot conditions, as presented in Fig. 1.

One considers a two-component mixture. Velocity distribution functions f_i of mixture components at both sides are Maxwellian, and their relative concentrations are the same. The problem consists of solution with the indicated initial conditions and fixed boundary conditions at $x = -L$ and $x = L$ of the system of Boltzmann equations:

$$\frac{\partial f_i}{\partial t} + \xi_i \frac{\partial f_i}{\partial x} = \sum_j (f_i' f_j' - f_i f_j) g_{ij} b d b d e d^3 \xi_j$$

The computation continues until the stabilization of the solution. When the steady state is reached, one computes a functional that determines the frequency of collisions exceeding some given energy threshold:

$$Q_R^{ij} = \int f_i f_j H(g_{ij} - g_R) b d b d e d^3 \xi_i d^3 \xi_j$$

Here $H(g_{ij} - g_R)$ is the Heaviside function, and g_R is the relative velocity defined by the given energy threshold. The gas parameters are calculated as well.

For accurate computations it is important to choose the appropriate discretization parameters. In Fig. 2 the graphics show the dependence of inverse SW thickness $\delta = \lambda_1 (dn/dx)_{\max} / (n_2 - n_1)$ on the coordinate step h_x / λ_1 and momentum mesh Δp^α for computation of $M = 3$ shock wave with equal concentrations $n^\alpha = n^\beta$ and mass ratio $m^\alpha / m^\beta = 1/2$. Molecular mean free path for molecules—rigid spheres of the radii b_0 —is defined as $\lambda_1 = 1 / \sqrt{2} \pi b_0^2 n_1$, where n_1 is the gas density before the

F. Tcheremissine (✉)
Dorodnicyn Computer Centre of RAS, Moscow, Russia
e-mail: tcherem@ccas.ru

O. Dodulad • Yu. Kloss
National Research Centre “Kurchatov Institute”, Moscow, Russia
Moscow Institute of Physics and Technology, Dolgoprudny, Russia

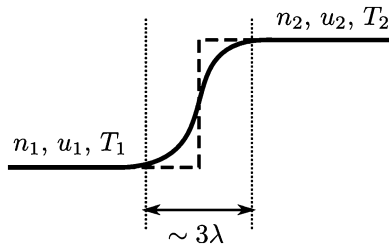


Fig. 1 Scheme of the shock wave computation

SW. The graphics show the quadratic convergence of computations by both parameters.

In Fig. 3 our computations of SW (lines) are compared with the results of Kyoto University team [8] (circles) obtained by a very intensive computations with the use of high-order polynomial approximation of the distribution functions in cylindrical coordinates. Molecular model of rigid spheres is used, Mach number $M = 3$. Two cases are presented: $m^\alpha/m^\beta = 1/4, n^\alpha = n^\beta$ (at the left) and $m^\alpha/m^\beta = 1/2, n^\alpha/n^\beta = 9$ (at the right). At the right graphic, T^β denotes the temperature of the second component. For both cases the agreement is excellent.

In Fig. 4 our results (lines) are compared with the experimental measurements [9] in helium–xenon mixture for two cases: (a) $M = 3.89$, 97 % of helium and 3 % of xenon (at the left), and (b) $M = 3.61$, 98.5 % of helium and 1.5 % of xenon (at the right). For the calculations we applied Lennard–Jones molecular potential with cross-sectional parameters $\sigma^{\text{He}} = 2.576\text{\AA}$, $\sigma^{\text{Xe}} = 4.055\text{\AA}$ and energy parameters $\epsilon^{\text{He}} = 10.2\text{K}$, $\epsilon^{\text{Xe}} = 229\text{K}$. For helium–xenon collisions, the potentials are defined by the combinatory relations $\sigma^{\text{He-Xe}} = (\sigma^{\text{He}} + \sigma^{\text{Xe}})/2$, $\epsilon^{\text{He-Xe}} = \sqrt{\epsilon^{\text{He}}\epsilon^{\text{Xe}}}$. The agreement is reasonably good, except the humps at the experimental graphics for helium.

Study of High-Energy Collisions

The computations were made for helium–xenon mixture with the above indicated molecular potentials. The molecular mass ratio for the mixture is $m^\alpha/m^\beta = m^{\text{He}}/m^{\text{Xe}} = 1/33$. In Fig. 5 the data for the case $M = 5, n^\alpha/n^\beta = 500$ are presented.

At the top graphic, reduced densities, temperatures, and longitudinal components of the temperature tensor are shown, and at the bottom graphic, the reduced values of the functional Q^{ij} which is defined as $Q^{i,j}(x) = \left(Q_R^{i,j}(x) - Q_R^{i,j}(L) \right) / \left(Q_R^{i,j}(L) - Q_R^{i,j}(-L) \right)$ for some chosen threshold velocity $g_R = 5\sqrt{(m_i + m_j)kT_2/(m_i m_j)}$, where T_2 is the temperature behind the SW, are given. It is seen that the maximal frequency of high-energy

xenon–xenon collisions overpasses the value in the hot zone behind the SW nearly by 35 times, and the maximal frequency of helium–xenon high-energy collisions are about 15 times higher the value in the hot zone. The functional $Q^{\alpha\alpha}$ is monotonous. It is important to remark that the location of the maximum of the frequency of high-energy xenon–xenon collisions coincides with the maximum of xenon longitudinal temperature T_{xx}^β .

In Fig. 6 the same functionals are computed under the assumption that the distribution functions of the components are locally ellipsoidal Maxwellian with the longitudinal temperatures $T_{xx}^i(x)$ and transversal temperatures $T_{rr}^i(x)$.

The graphics show that qualitatively the overshoot of $Q^{\beta\beta}$ functional can be explained by the longitudinal extension of the corresponding distribution function, without the assumption of its bimodal structure. At some extend, this is also true for $Q^{\alpha\beta}$ functional, but not for $Q^{\alpha\alpha}$. This observation is confirmed in Fig. 7 that presents longitudinal slides of the distribution functions at different locations. The distances in the figure are expressed in molecular mean free path before the SW, whose center is at $x = 0$ and v_0 is the mean thermal velocity of the mixture. The examination of the distribution function f^α for the light gas shows a small bimodal structure at $x = 0$, but not elsewhere. The function f^β for the heavy gas doesn't have the noticeable bimodal structure, but one can observe the gradual extension of the distribution from $x = 25$ to $x = 9$. The maximum of high-energy collisions is located just near $x = 9$ in the area of the largest extension of the function f^β in the longitudinal direction.

The computations for the same Mach number in different concentration ratio were performed as well. For the case $n^{\text{He}}/n^{\text{Xe}} = 50$, only the excess of the frequency of xenon–xenon high-energy collisions, which is of about two times by the value, was found, when the frequencies for helium–xenon and helium–helium high-energy collisions are monotonous. For equal concentrations of the mixture components, all the functionals are monotonous, and the considered phenomenon is absent.

Conclusions

The phenomenon of the excess of high-energy collisions inside the shock wave in a gas mixture with large difference of molecular masses of the components was confirmed in the case when the heavy component presents a small fraction by accurate solution of the Boltzmann kinetic equation. In addition, it was found that the origin of the phenomena lies in the longitudinal extension of the distribution function for the heavy gas, but not in the bimodal structure of the function. Details of the analysis are published in the electronic form [10].

Fig. 2 Parametric study of the convergence of the solution

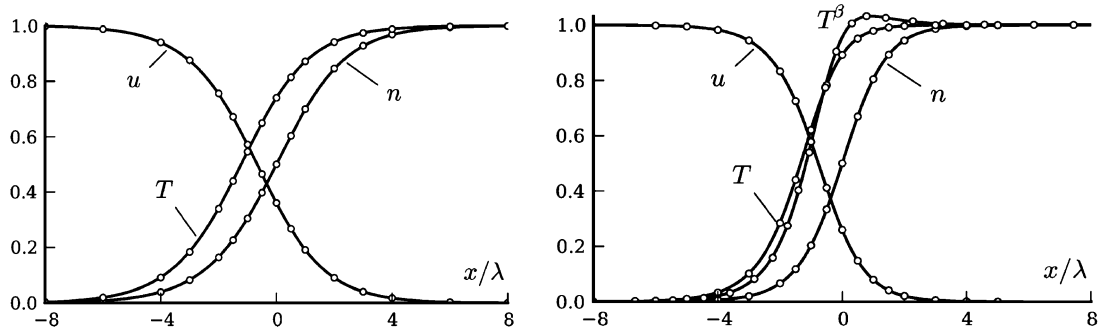
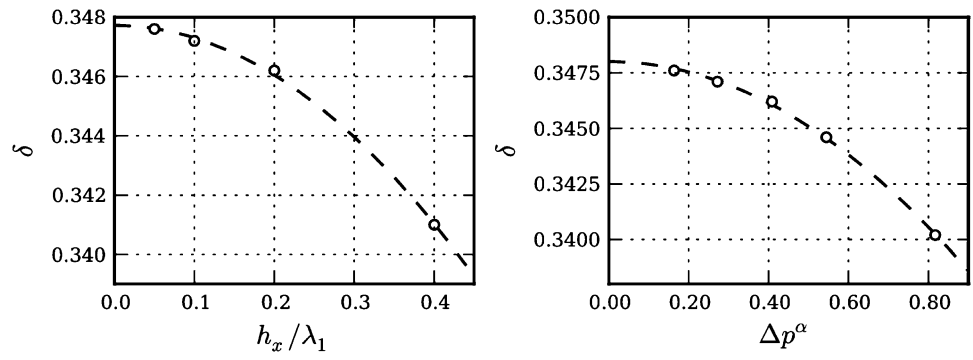


Fig. 3 Comparison with computations by Kyoto team

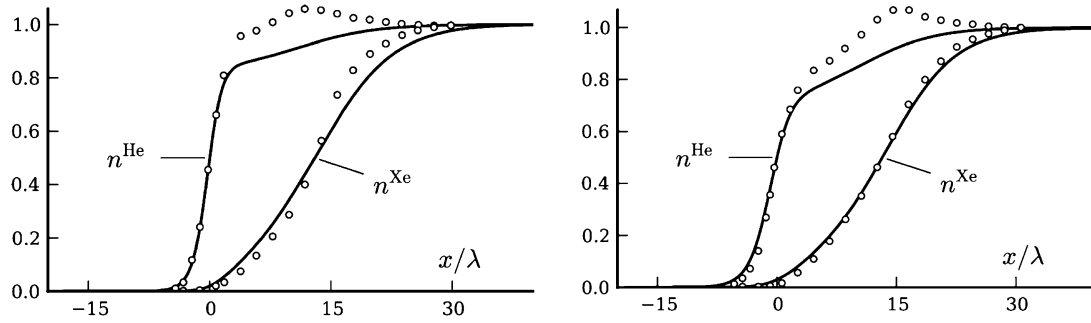


Fig. 4 Comparison with experimental data

Fig. 5 Gas parameters and high-energy collision frequencies of the mixture components

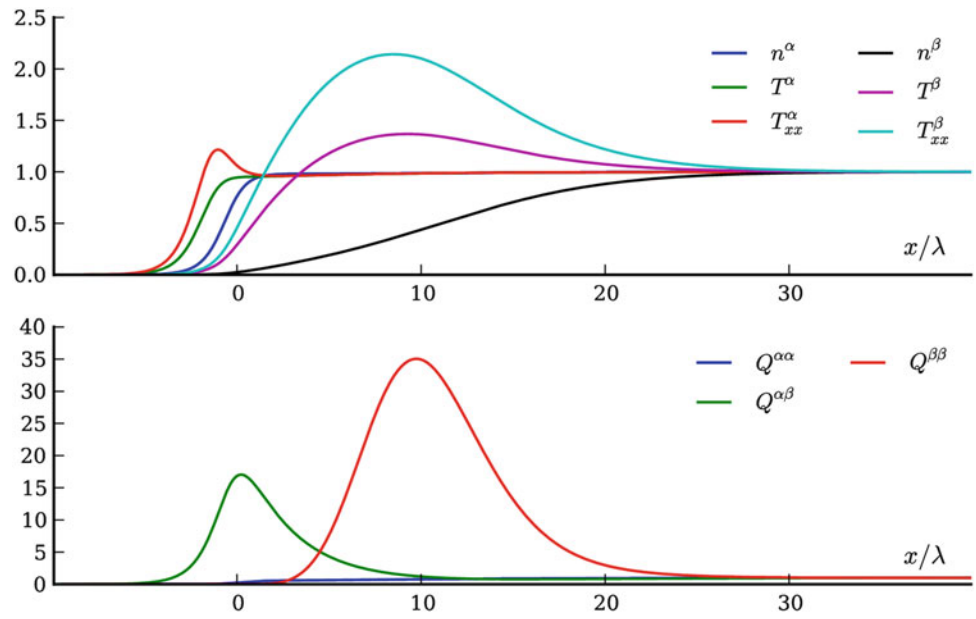


Fig. 6 Frequencies of high-energy collisions for locally Maxwellian distribution functions

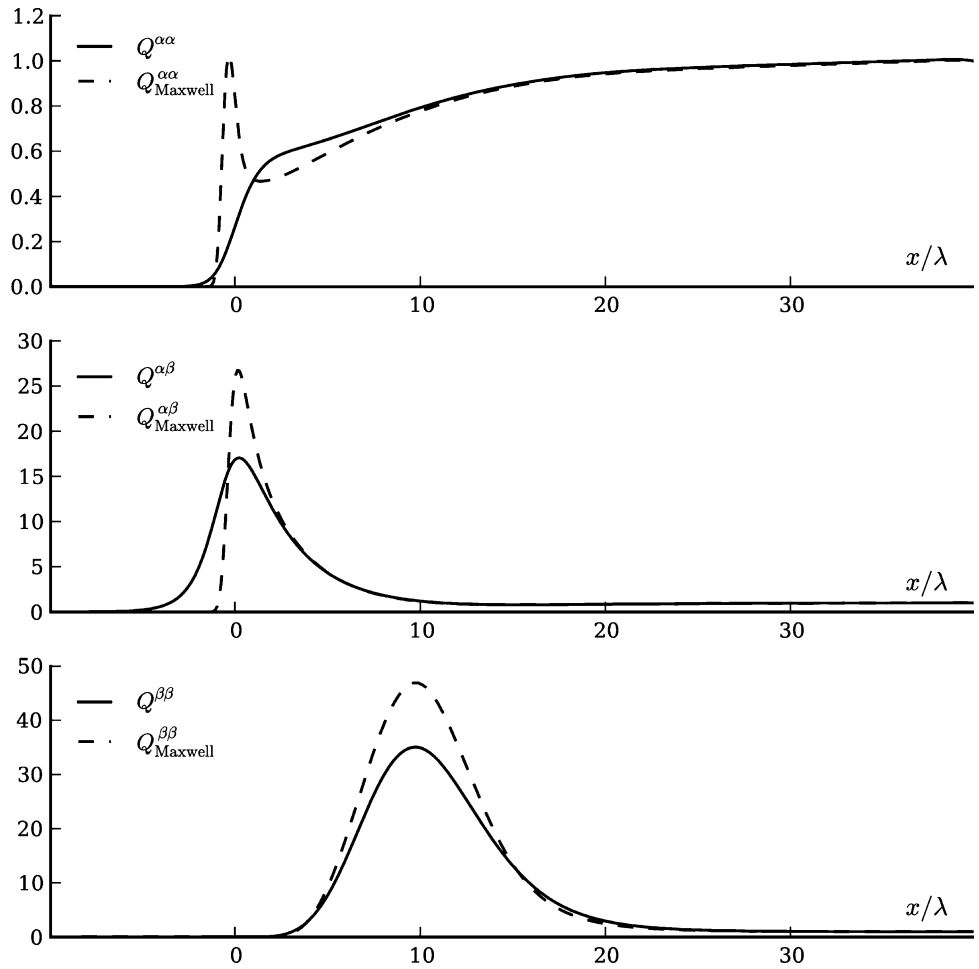
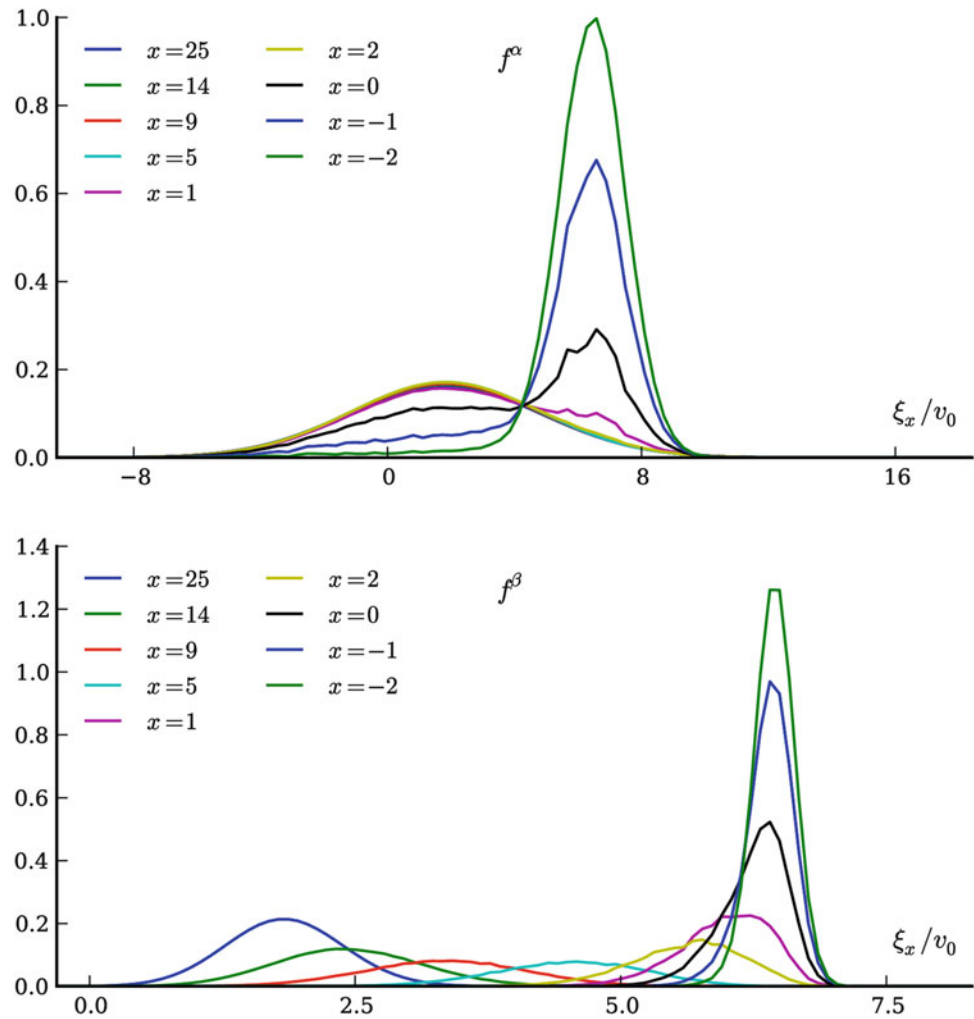


Fig. 7 Distribution functions of the mixture components at different locations



References

1. Velikodnyi, V.Y., Emel'yanov, A.V., Eremin, A.V.: Nonadiabatic excitation of iodine molecules in the translational disequilibrium zone of a shock wave. *J. Tech. Phys.* **44**(10), 1150–1158 (1999) (in Russian)
2. Emel'yanov, A.V., Efremov, V.P., Zaborov, V.S., Fortov, V.E., Shumova, V.V.: Ionization in the front of a weak shock wave with a small admixture of molybdenum hexacarbonyl. *Physical-Chemical Kinetics in Gas Dynamics*. www.chemphys.edu.ru/pdf/2007-07-26-001.pdf (2007) (in Russian)
3. Kulikov, S.V.: Evolution of the tails of velocity distributions for gas mixtures inside the shock wave and the influence of the non-equilibrium state at the reaction of H_2 with O_2 . *Math. Model.* **11**(3), 96–104 (1999) (in Russian)
4. Kulikov, S.V.: Modeling of the acceleration of chemical reactions in a shock front. *J. Fluid Dyn.* **36**(5), 827–835 (2001)
5. Emel'yanov, A.V., Eremin, A.V., Kulikov, S.V.: On the origin of the non-equilibrium radiation of the iodine molecules in the shock wave front. *J. Tech. Phys.* **83**(5), 24–29 (2013) (in Russian)
6. Tcheremissine, F.G.: Conservative method of evaluation of the Boltzmann collision integral. *Dokl. Phys.* **357**, 53–56 (1997)
7. Dodulad, O.I., Tcheremissine, F.G.: Multipoint conservative projection method for computing the Boltzmann collision integral for gas mixtures. In: 28th International Symposium on Rarefied Gas Dynamics. AIP Conference Proceedings, vol. 1501, pp. 302–309 (2012)
8. Kosuge, S., Aoki, K., Takata, S.: Shock-wave structure for a binary gas mixture: finite-difference analysis of the Boltzmann equation for hard-sphere molecules. *Eur. J. Mech. B Fluids* **20**(1), 87–126 (2001)
9. Gmurczyk, A.S., Tarczynski, M., Walenta, Z.A.: Shock wave structure in the binary mixtures of gases with disparate molecular masses. In: 11th International Symposium on Rarefied Gas Dynamics, vol. 1, pp. 333–341 (1978)
10. Dodulad, O.I., Kloss, Y.Y., Tcheremissine, F.G.: Computing of the shock wave structure in a gas mixture on the base of solution of the Boltzmann equation. www.chemphys.edu.ru/pdf/2013-070-08-001.pdf (2013) (in Russian)